NEUROMORPHIC VESTIBULAR SYSTEM

Modeling regular and irregular afferents on the Dynap-se1 chip

Naima Elosegui Borras, Anja Šurina

Neuromorphic intelligence 2021 class project

Contents

1 Introduction

The human vestibular system is composed of the otolith organs and the semicircular canals, that in conjunction encode head position and velocity relative to space. The otolith organs encode linear acceleration and translation in space, whereas the semicircular canals encode angular velocity. Both the otolith organs and the semicircular canals sense movement through afferents in hair cells in the vestibular system [4] [2]. Vestibular afferents are classified as either regular or irregular based on resting discharge as well as morphology [3]. Regular afferents use temporal codes to transmit information about the detailed time course of the stimulus, whereas irregular afferents best code for high frequencies using rate encoding. Consistent with this theory, regular afferents have 50% lower angular velocity thresholds than irregular ones. More differences are stated in the table in Figure 1.

REGULAR AFFERENTS	IRREGULAR AFFERENTS
lower gains	higher gains
lower angular velocity detection threshold (4°/s)	higher angular velocity detection threshold (8°/s)
severely affected by spike-timing jitter	less sensitive to spike-timing jitter
transmit info about detailed time course of the stimulus	best encode high frequencies
lower variability	higher variability
temporal code	rate code

Figure 1: Table 1: Key differences between regular and irregular afferents

2 Materials and methods

2.1 Dynap-se1

To model the vestibular system afferents, we used the Dynap-se1 neuromorphic chip. Each Dynap-se1 box contains 4 chips and each chip contains 4 cores. There are 256 neurons in each core, thus there is a total of 1024 neurons in a single chip. Each neuron can be excited/inhibited through a synapse by spikes from other neurons or from spike generators. Another form of stimuli is direct current, which is injected directly into the neurons. We used 14 neurons in the chip to represent 14 regular afferents. For the irregular afferents, we used a network of 21 neurons, 14 of them excitatory and 7 inhibitory. The inhibitory population was used only to model the intrinsic noise of the irregular afferents.

2.2 Random uncorrelated noise

In the vestibular system irregular neurons differ from regular neurons by their resting discharge. Particularly, irregular neurons demonstrate higher variability or noise compared to regular neurons in the absence of stimuli [2] . The noise between neurons is uncorrelated, thus to model this property in irregular neurons we randomly connected excitatory and inhibitory neurons. Following the approach by *Chicca et al.,* [1] to generate a stochastic network, we created a neuron population with 14 excitatory neurons and 7 inhibitory ones. Each neuron was connected randomly to another 7 neurons in the population, avoiding self connections. The connectivity diagram obtained was as depicted in Figure 2. We used GABAb synapses to connect the inhibitory neurons to the excitatory ones and AMPA synapses to connect excitatory to inhibitory neurons. Excitatory neurons were connected amongst themselves with NMDA synapses.

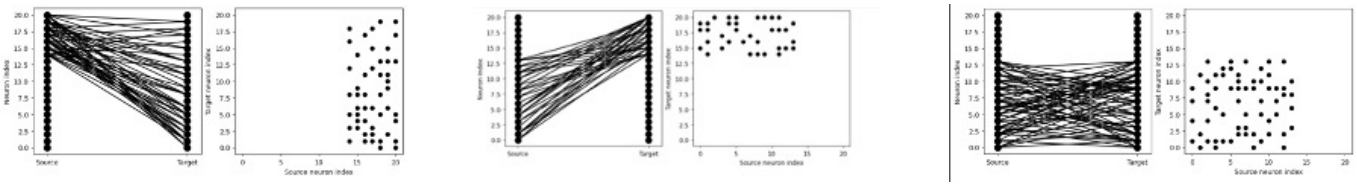

(a) Inhibitory neuron random connections

(b) Excitatory to inhibitory connections

(c) Excitatory to excitatory connections

Figure 2: Connectivity between irregular neurons creating random uncorrelated noise within the population. Note that our network does not have two layers but just one, in the diagrams the neurons are repeated for easier visualization.

2.3 Head-direction signal

To test how head rotational input affects the behaviour of the irregular and regular neuron populations, we generated a random broadband head velocity stimulus, ranging from 0-20 Hz, mimicking typical head rotation. Following the methodology of *Sadeghi et al.,* to construct the random stimulus we sampled a Gaussian distribution with mean 0 and standard deviation of 20°/s. This signal was then low-pass filtered with a 10th order Butterworth filter with a cutoff frequency of 30 Hz. The input unfiltered and filtered signals can be seen in Figure 3.

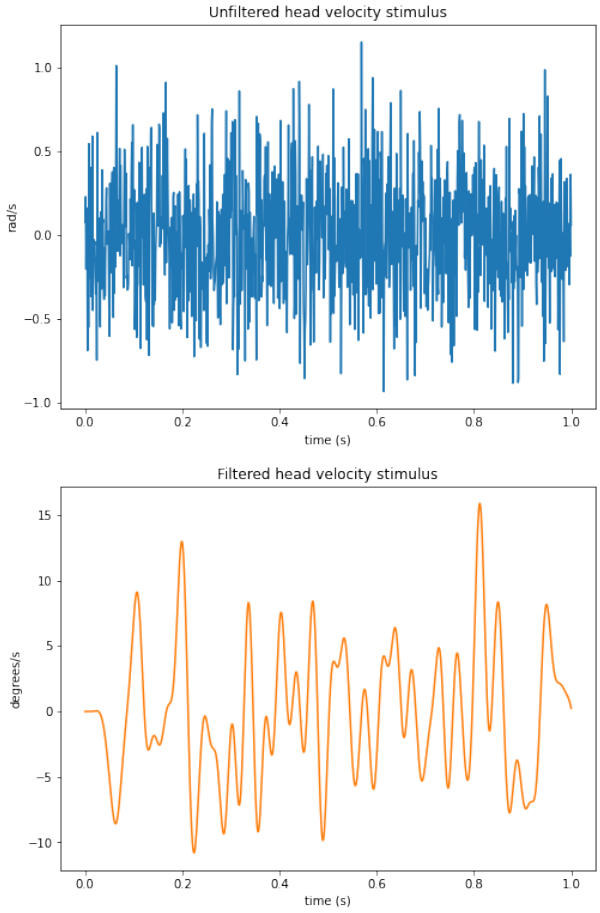

Figure 3: Head velocity stimulus generated from a Gaussian distribution. The upper plot demonstrates the original signal, and the bottom plot shows the stimulus low-pass filtered at 30 Hz.

2.4 Pulse frequency modulation

Once the signal was produced, we converted it into digital spikes by first transforming it using pulse frequency modulation [5]. Pulse frequency modulation was performed by multiplying the low-passed input signal by a carrier frequency sine wave of 60 Hz. We selected this carrier frequency as it is biologically plausible when taking into

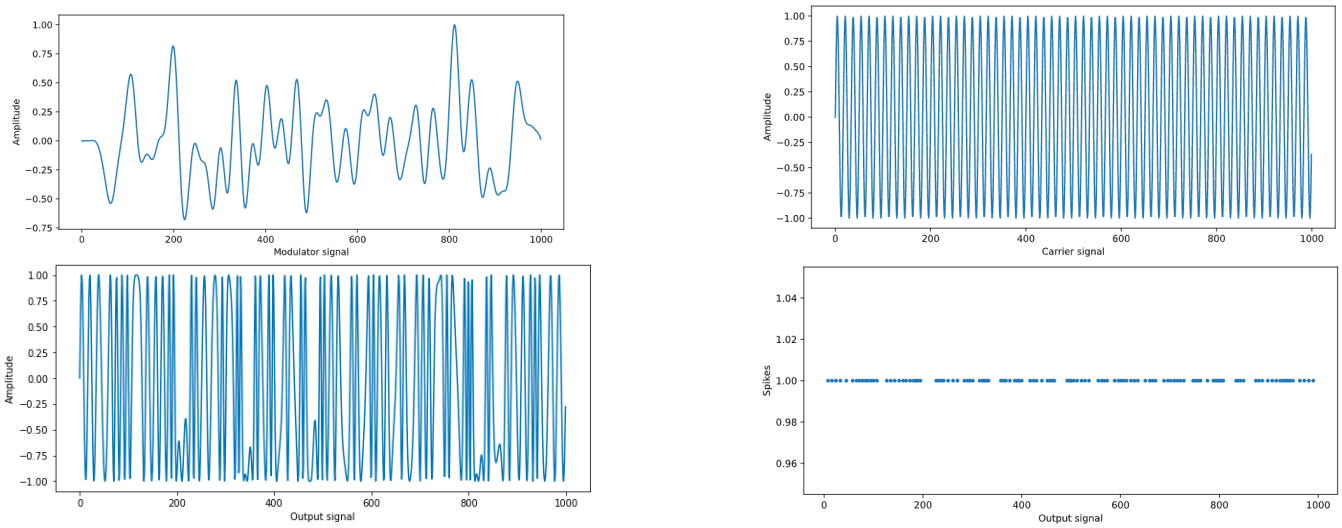

Figure 4: Pulse frequency modulation and conversion to spikes

consideration neuronal firing rate. The step-by-step computation can be visualized in Figure 4. Finally, we found the spike times within the stimulus duration by taking the zero crossings of the product signal.

2.5 Sigma delta modulation

The other type of encoder we utilized was the adaptive sigma-delta modulator [6]. Whereas pulse frequency modulation takes into account the amplitude of the signal, sigma delta modulation considers how the signal changes. When the signal follows an upward slope, spikes "up" are produced and when the signal follows a downward slope, spikes "down" are produced. If the changes in the signal are not big enough, no spikes are produced. The "up" and "down" spikes we obtained for the head stimuli can be seen in Figure 5.

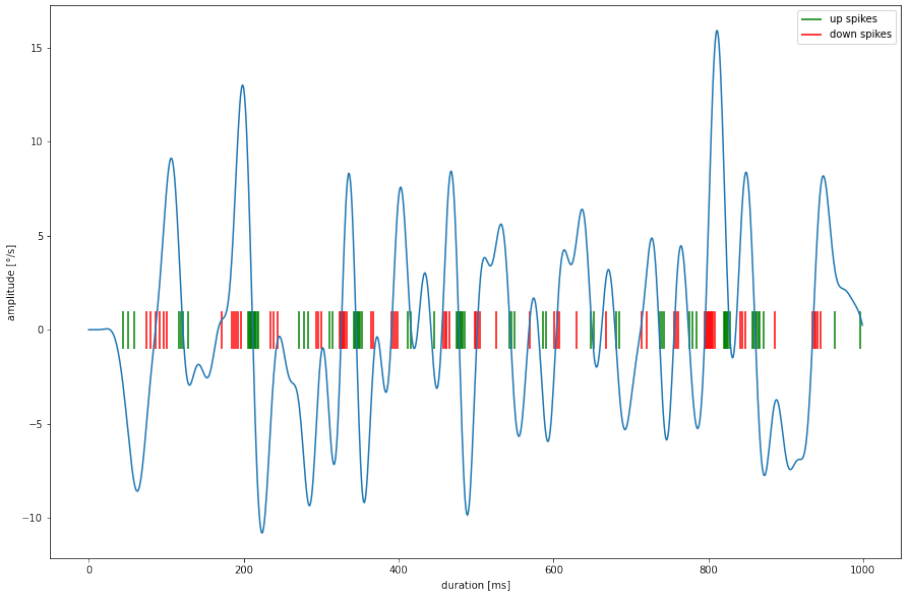

Figure 5: "Up" and "down" spike trains obtained using sigma delta modulation

2.6 Signal reconstruction

We monitored Dynap-se1 neurons and recorded their responses to the stimuli. To reconstruct the signal we convolved the spike train of the first neuron (index 0) with a kernel. Convolution was done in the time domain:

$$s_{\text{est}}(t) = \int K(\tau) r(t-\tau)\, d\tau \tag{1}$$

where $s_{est}(t)$ denotes the reconstructed (estimated) signal, $K(\tau)$ is the kernel and $r(\tau)$ is the spike train response of the neurons.

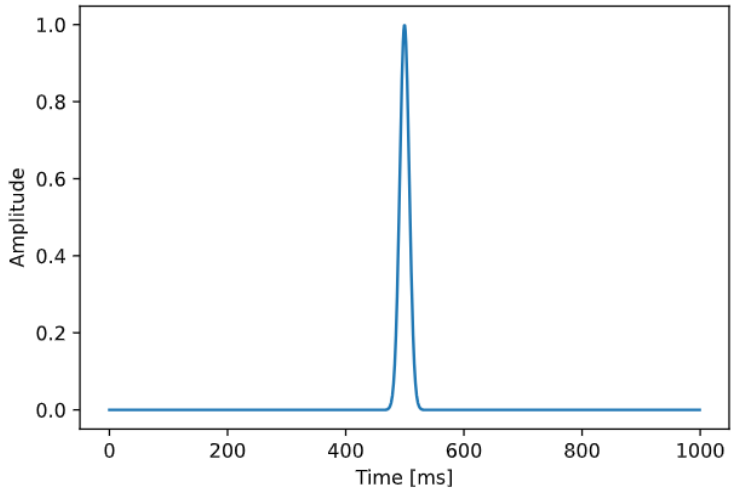

Figure 6: Monophasic kernel

When stimuli was encoded using pulse frequency modulation, we used two types of kernels. For the regular neurons we used a Gaussian kernel with SD = 8. The kernel was monophasic in this case, as depicted in Figure 6. For the irregular neurons we used a biphasic kernel, comprised of two Gaussians with mean = 0 and SD=7. The kernels were shifted and concatenated, to have the change in Guassian centered at 500ms as shown in Figure 7. We used the kernels of this type as an approximation of the ones used by *Sadeghi et al.,*. When the stimuli was encoded using sigma delta modulation, we used the biphasic kernel for both regular and irregular neurons. We decided for this kernel because sigma-delta encodes positive and negative changes in the signal and using a biphasic kernel can give us not only positive but also negative values, which is not possible with a monophasic kernel.

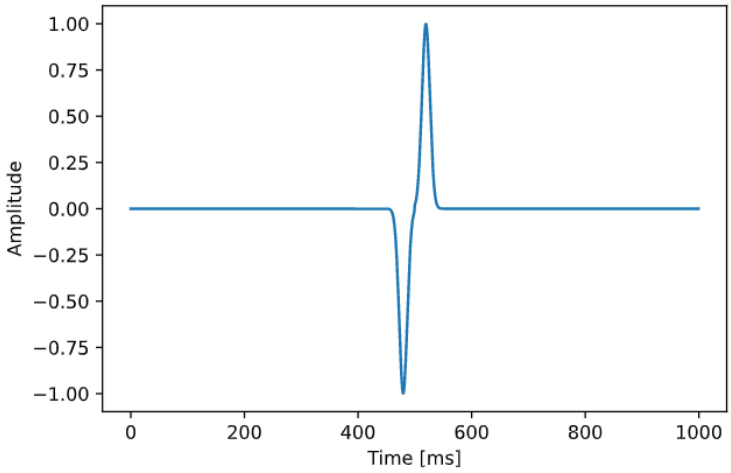

Figure 7: Biphasic kernel

2.7 Reconstruction quality

To compare the input head velocity signal and the output reconstructed signal, we looked at their correlation score. Firstly, we normalized both signals to be in the range between [-1,1] and then we computed Pearson's correlation coefficient. The normalization does not affect correlation and was purely for visualization purposes. As the resulting signal reconstruction is generated by convolving a kernel and the output spike train, it includes more data points in time, thus we shifted the reconstruction signal to where the output was encoded.

2.8 Project code

The GitHub repository for this project can be found at: https://github.com/naimaeb/Vestibular-system-project.

3 Results

3.1 Non-stimulus response

To model the non-stimulus response we injected direct current into the neurons. Spike generators were turned off for the whole duration of the experiments. For the regular neurons, current was the only form of excitation. Irregular neurons were additionally excited/inhibited by spikes from other neurons in the network. As shown in Figure 10, regular neurons had consistent inter-spike intervals. On the other hand, modeling the intrinsic noise in irregular neurons by random connections resulted in higher variability of inter-spike intervals. While ISI histograms looked similar for all regular neurons, there was more variability in the ISI histograms of the irregular neurons. We strove to tune the Dynap-se1 parameters in a way that the ISI histograms of Figure 5 (recorded from neurons in Dynap-se1) would look as similar as possible to the ISI histograms of Figure 4 (recorded from neurons in vestibular system of macaque monkeys [3]).By comparing the power spectra of regular neurons with data from Dynap-se1 and macaque monkeys, we can see that both contain peaks at 100Hz and its integer multiples (harmonics), even though the peaks for the Dynap-se1 data are less prominent.

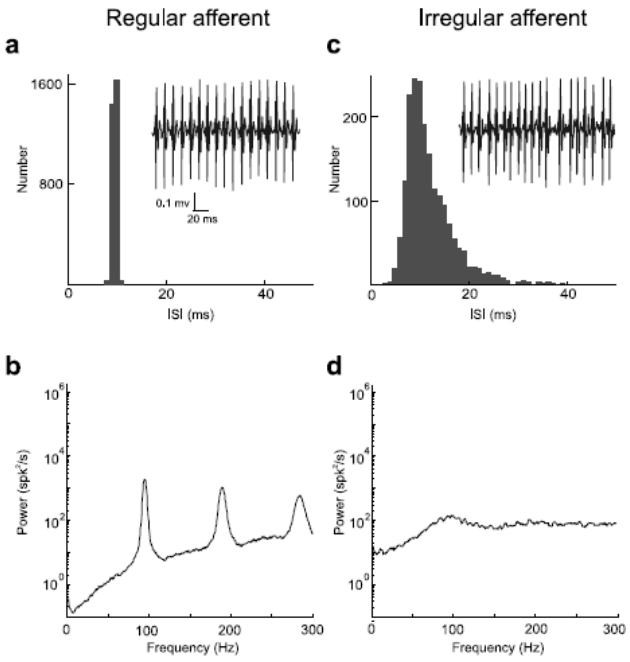

Figure 8: Spontaneous activity of typical regular and irregular afferents. The data was recorded from the vestibular system of macaque monkeys [3]. a) Inter-spike interval from a typical regular afferent. b) Spike train power spectrum for the regular afferent. c) Inter-spike interval from a typical irregular afferent. d) Spike train power spectrum for an irregular afferent.

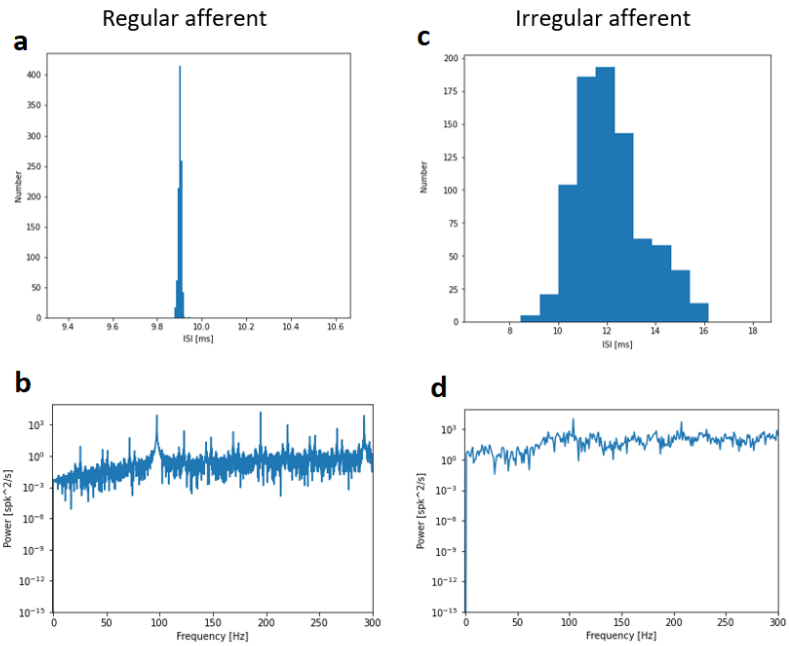

Figure 9: Data recorded from the Dynap-se1 chip for the non-stimulus experiments. a) Interspike interval from a regular afferent. b) Spike train power spectrum for the regular afferent. c) Interspike interval from a irregular afferent. d) Spike train power spectrum for an irregular afferent.

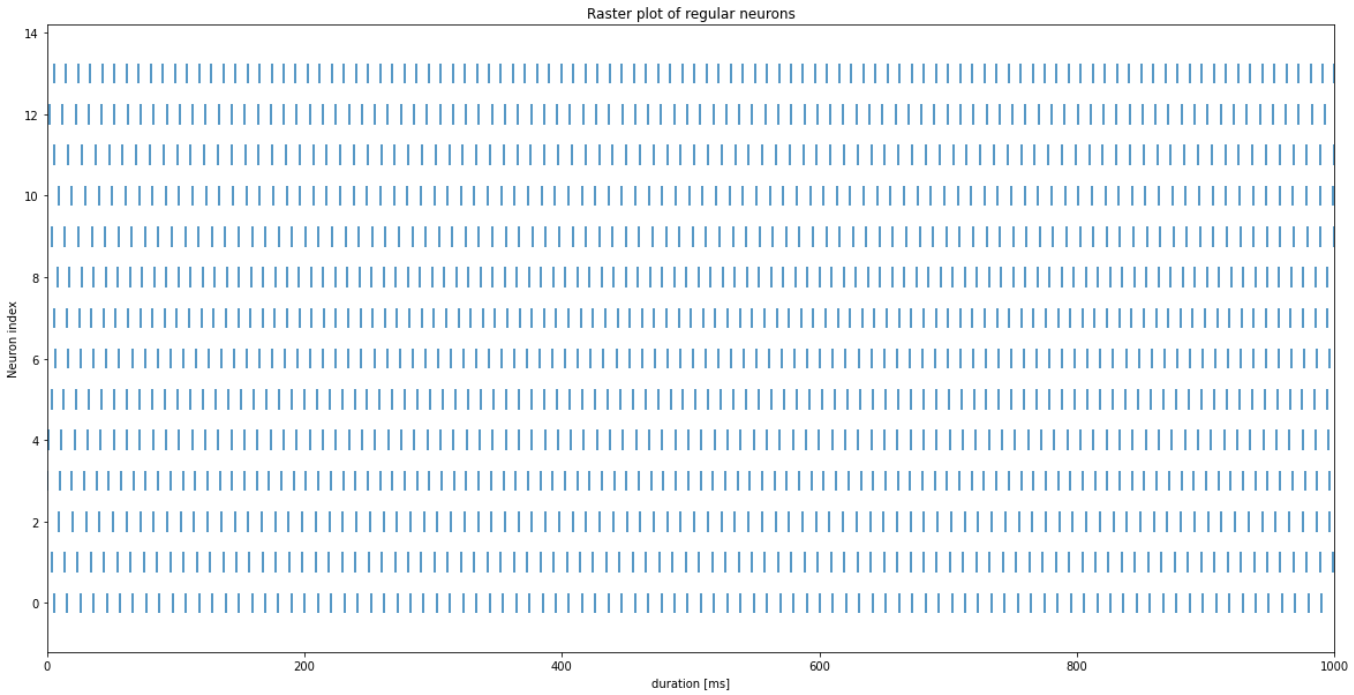

Figure 10: Raster plot of the regular neurons during the non-stimulus experiments.

3.2 Response to pulse frequency encoded head velocity stimulus: regular neurons

To analyse the behaviour of the regular neuron population, we used a random head velocity stimulus lasting 1 second, as specified in the methods section in Figure 3. After inputting the signal and recording the response for the duration of the signal (1 second), we obtained the spike train observed in Figure 12 for the 14 regular neurons.

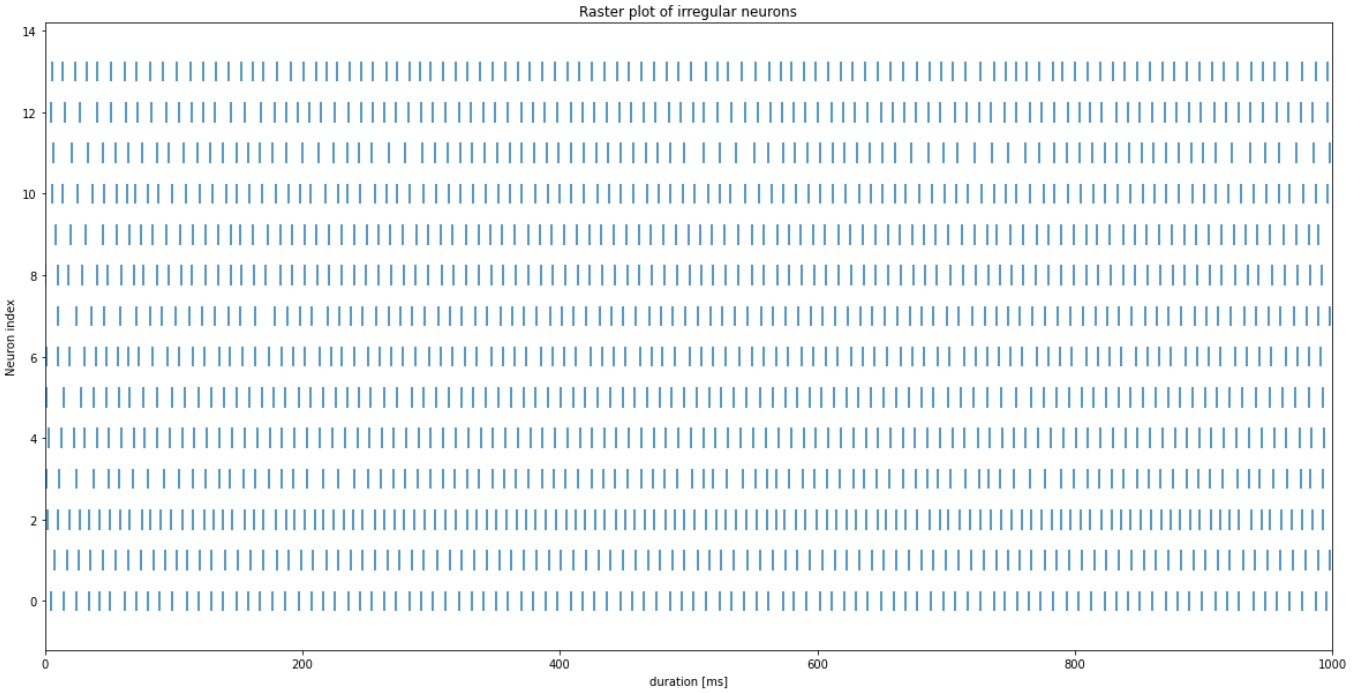

Figure 11: Raster plot of the irregular neurons during the non-stimulus experiments.

To convert the spike train back into a head velocity sinusoid, we convolved the spike train with a monophasic Gaussian kernel as described in the Methods section and visualized in Figure 6. After normalizing both signals we calculated the correlation coefficient of the stimulus and output to be 0.72, correct to two decimal places. Figure 13 depicts the superposition of the original head velocity stimulus and the reconstructed output signal for one neuron in the population, namely neuron 0.

3.3 Response to pulse frequency head velocity stimulus: irregular neurons

Inputting the pulse frequency encoded head velocity signal described above into the irregular neuron population lead the neurons to respond as seen in Figure 14.
After reconstructing the output signal from the spike train and normalizing it, we calculated Pearson's correlation coefficient for the input stimulus and the output. For neuron 0 in the population we got a correlation coefficient of 0.37, correct to two decimal places. The overlay of the normalized stimulus and reconstruction is shown in Figure 15.

3.4 Response to sigma delta encoded head velocity stimulus: regular neurons

To analyze the responses of neurons to sigma-delta encoded stimuli we used the same procedure as in the pulse frequency modulation experiments. The only difference was that this time we used the biphasic kernel for irregular as well as regular neurons. The raster plot of the regular neurons is shown in Figure 16. The Pearson correlation coefficient was 0.52 for the regular neurons.

3.5 Response to sigma-delta encoded head velocity stimulus: irregular neurons

The responses of the irregular neurons to the sigma-delta encoded stimuli are shown in Figure 18. In this experiment we computed a Pearson correlation coefficient of 0.55.

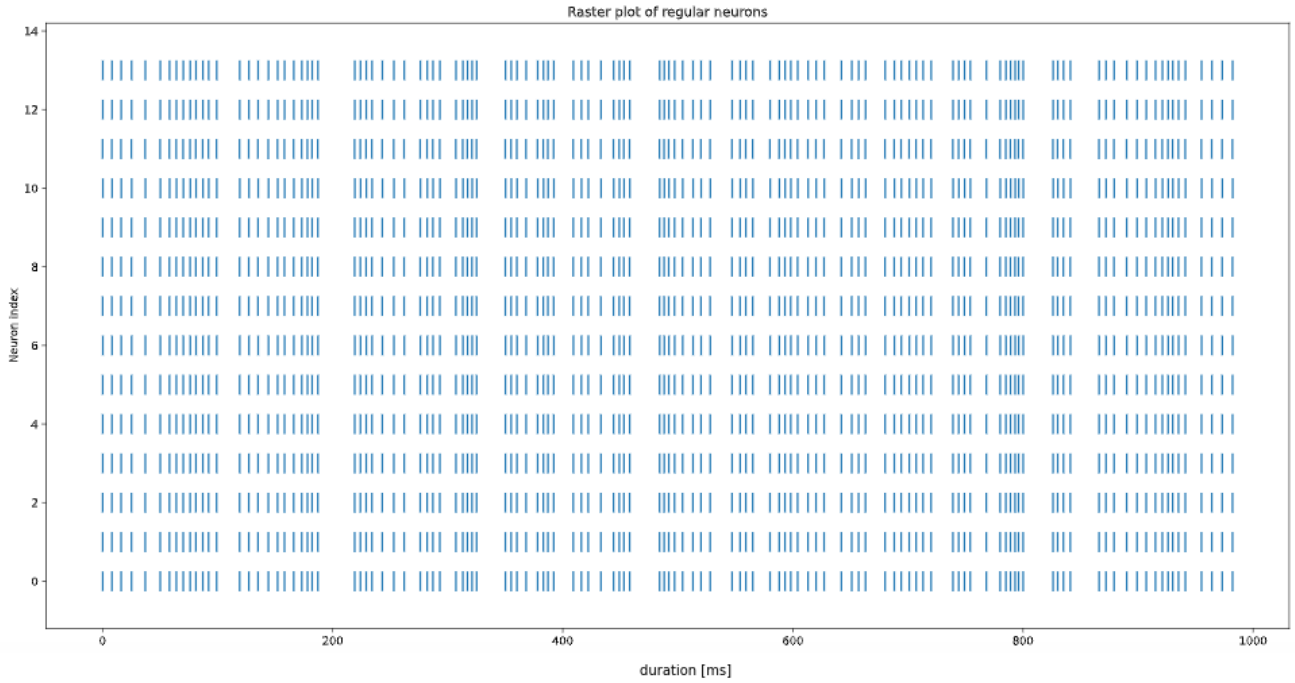

Figure 12: Raster plot of the regular neurons for the pulse frequency encoded head velocity stimuli experiment

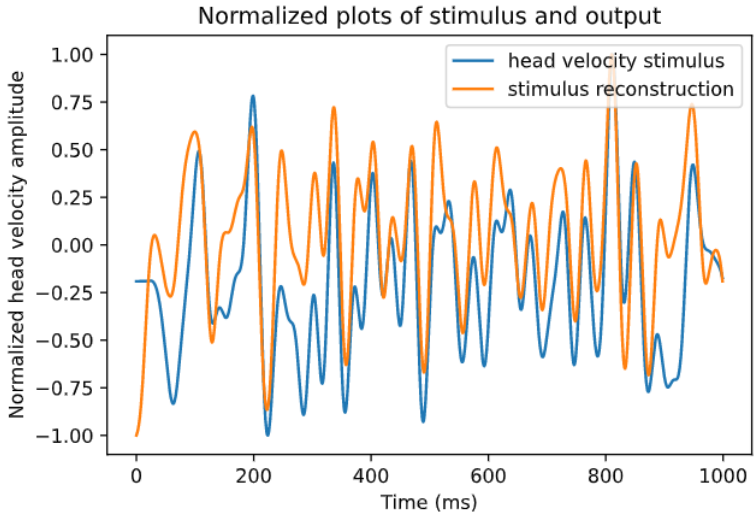

Figure 13: Comparison between the input stimulus and the reconstruction for the regular neuron. Stimulus was encoded using the pulse frequency modulation.

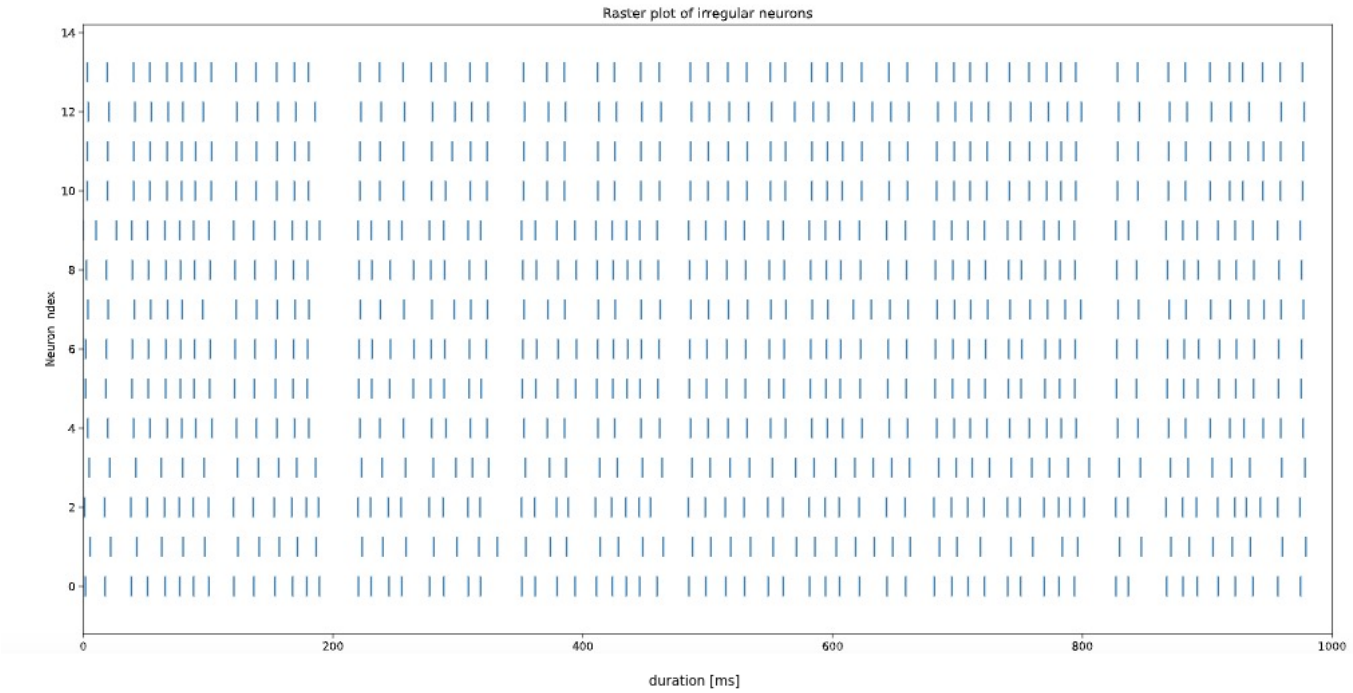

Figure 14: Raster plot of the irregular neurons for the pulse frequency encoded head velocity stimuli experiment

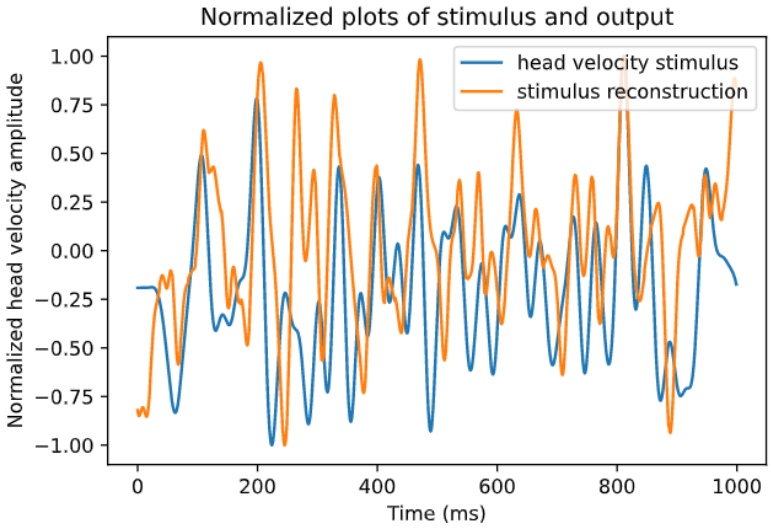

Figure 15: Comparison between input stimulus and the reconstruction for the irregular neuron. Stimulus was encoded using the pulse frequency modulation.

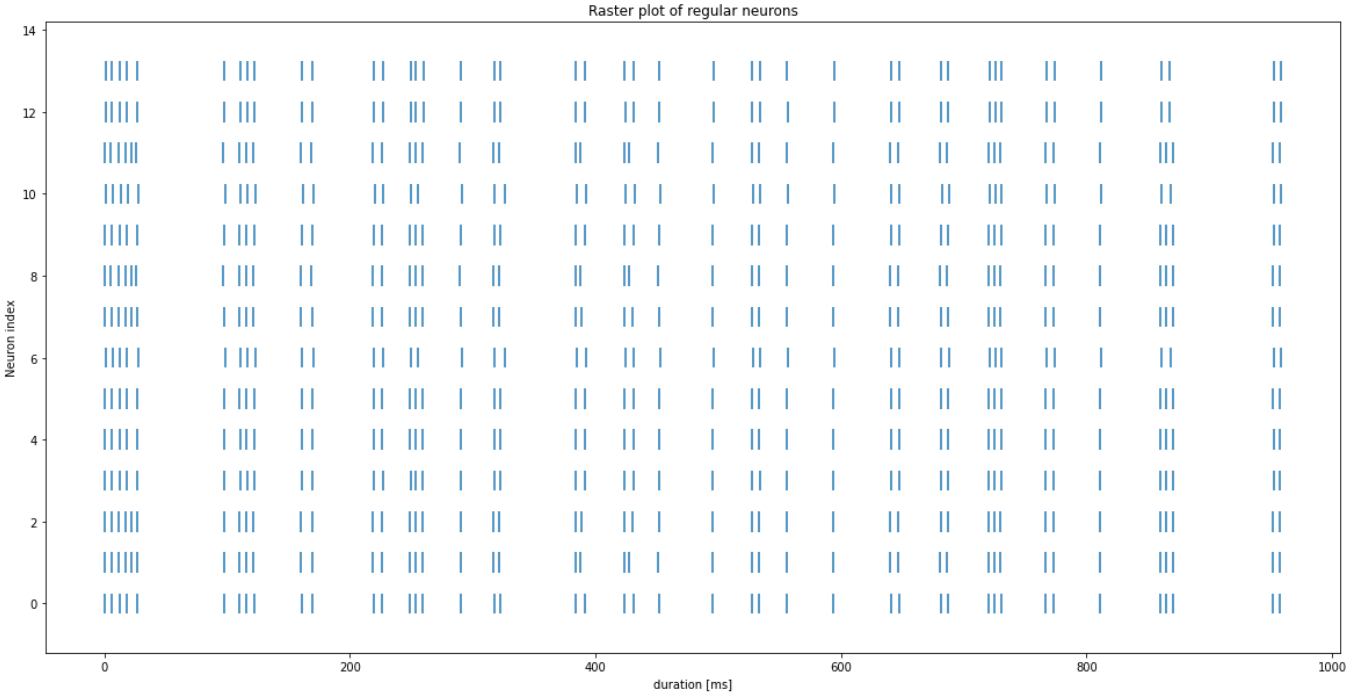

Figure 16: Raster plot of the regular neurons for the sigma-delta encoded head velocity stimuli experiment

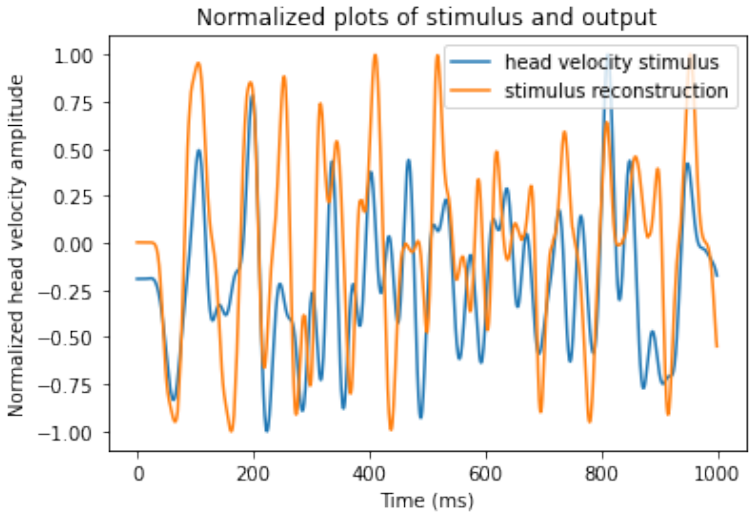

Figure 17: Comparison between the input stimulus and the reconstruction for the regular neuron. Stimulus was encoded using the sigma delta modulation.

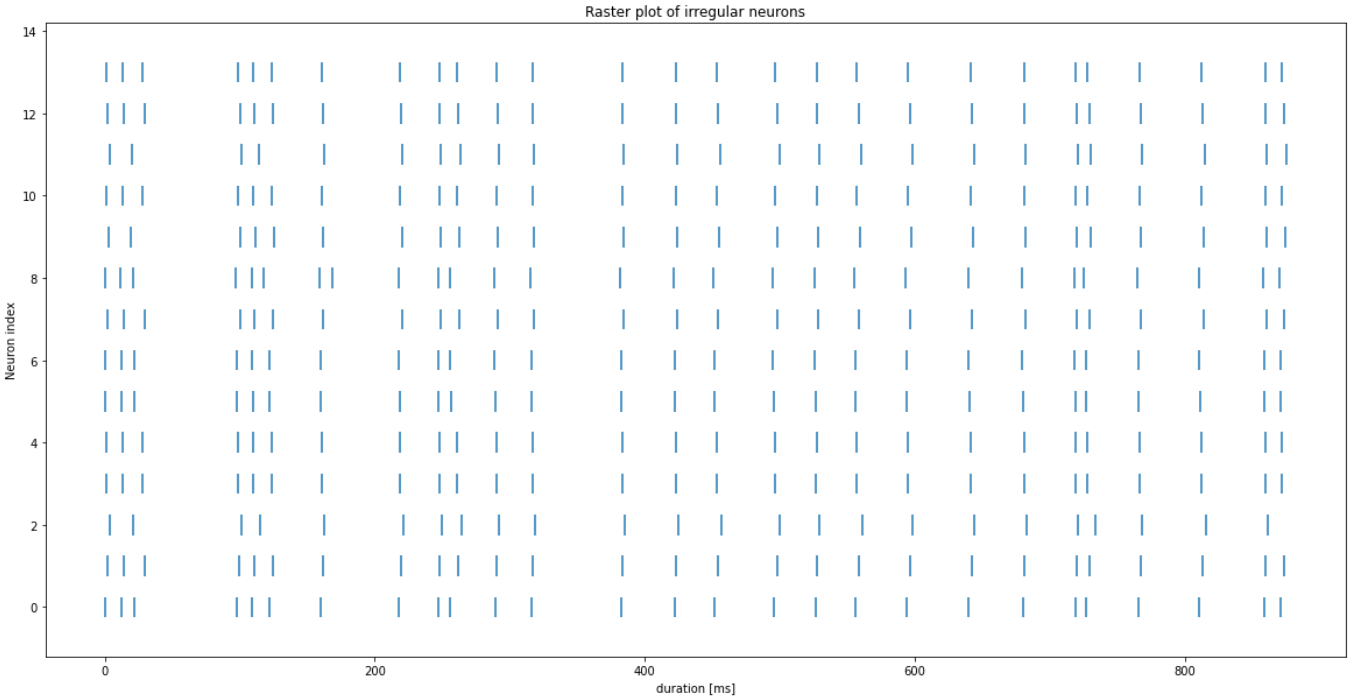

Figure 18: Raster plot of the irregular neurons for the sigma-delta encoded head velocity stimuli experiment

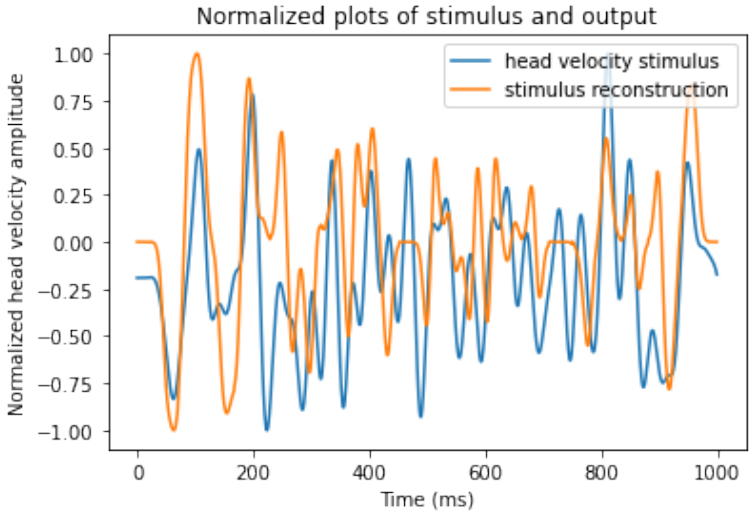

Figure 19: Comparison between the input stimulus and the reconstruction for the irregular neuron. Stimulus was encoded using the sigma delta modulation.

4 Discussion

Following the experimental approach of *Sadeghi et al.,* we probed whether the regular and irregular neuron populations could exhibit biologically-similar firing rates to mimic the vestibular system.
When no input was given to the neurons, both the regular and irregular neurons demonstrated inter-spike-interval distributions similar to those observed in biological neurons. As expected, the distribution of ISI's in irregular neurons has higher variability than that of regular neurons. This behaviour is due to higher noise in irregular neurons than in regular ones.
Furthermore, when observing the raster plots of the intrinsic firing of the neuron population, the pattern of regular neurons seems to be uniform across neurons and within neuron firing times. The raster plot of irregular neurons displays more variability within individual neuron firing times. Moreover, the firing pattern in the population is different across neurons, accounting for the higher variability in the ISI plots.

Once we had the silicon neurons tuned to the non-stimulus case, we connected them to the FPGA spike generators. Spike generators stimulated the neurons with spike trains encoding head direction stimuli. After monitoring the neurons we reconstructed the signal from the spike trains. To reconstruct the signal we tried three different approaches. Firstly, we tried the approach that was used by *Sadeghi et al.,* [3]. There, the response of neurons is convolved in the time domain with a kernel that minimizes the mean square error between the stimulus and the stimulus reconstruction. The kernel $K(\tau)$ is computed in the Fourier domain by dividing the cross spectrum and the power spectrum of the response as follows:

$$\widetilde{K} = \frac{P_{\mathrm{rs}}(-f)}{P_{\mathrm{rr}}(f)} \tag{2}$$

where $\mathrm{P_{rs}}$ denotes the stimulus-response cross spectrum, $\mathrm{P_{rr}}$ is the power spectrum of the spike train and $\widetilde{K}$ is the Fourier transform of the kernel. However, this approach did not give us good reconstruction accuracy. The most probable reason is that this approach might only work when the stimulus is injected into the neurons as a current and is not already encoded in spikes.
The second approach we used was spike-time binning to compute frequency. We divided the time points into bins, counted the amount of spikes in each bin and converted the result to frequency. However, this approach was too crude to be successful.
The approach that finally gave us best results was convolving the neuron spike-train response with a Gaussian kernel. The convolution was done in the time domain with kernels as described in *Materials and methods*.

By inputting the random head velocity signal into the irregular and regular neuron populations and computing the reconstruction from the output spike train, we determined how each neuron population encodes angular velocity stimuli. To determine whether our irregular and regular neurons encode stimuli as a change in amplitude or as amplitude values, we compared the reconstruction obtained by encoding the stimulus using the adaptive sigma-delta modulator to that of the pulse-frequency modulator.
When using the pulse-frequency modulator, that encodes the value of the amplitude, we obtained higher reconstruction values for regular neurons and lower for irregular, when comparing to sigma-delta modulation. From the raster plot of the regular neurons, we can observe that the neuron population spikes resemble input spike times. Moreover, when we compare the reconstructed response to the stimuli, we obtain a high correlation coefficient (0.72). The high similarity between input and output was expected, yet the firing pattern observed in the rater plot should be more regular to resemble that of biological neurons, as seen in *Sadeghi et al.,*. Nevertheless, we hypothesize that to have a high reconstruction correlation, the output spikes should be mimicking the input, thus it would not be possible to obtain a perfect reconstruction while observing uniform firing patterns. It is important to note that we did not introduce random uncorrelated noise in our regular neuron population. We hypothesize that introducing noise into the regular neuron population would lead to more regular firing, as the output spike train would be less driven by the exact dynamics of the input spike train. One of the future directions of this project would be to introduce random uncorrelated noise in the regular neuron population to make it more biologically plausible. To do so, one could follow the random connectivity approach described in the *Materials and methods*, but instead of 7 random connections, as in the irregular neurons, introduce 2 or 3 to have less noise than in the irregular neurons. In the case of irregular neurons, our results when using pulse-frequency modulation resemble those of biological vestibular neurons. As observed in the raster plot in 14, the neurons fire at a higher frequency when the amplitude of the head velocity is larger and lower when the velocity decreases. The correlation of the reconstruction with the input signal was low (0.37), as depicted in 15. This makes sense biologically, as irregular neurons encode high angular velocity frequencies and not all the angular velocity information generated by rotational head movements. This afferent was significantly less apt

at reconstructing the detailed time course of the head velocity signal, as predicted from the biological data.

The adaptive sigma-delta modulator approach to encode the stimulus lead to a higher reconstruction correlation for irregular neurons and lower for regular ones, when comparing to pulse-frequency modulation. From these results we hypothesize that irregular neurons encode high-frequency head rotation by looking at the changes in amplitude of the stimulus, whereas the regular encode the amplitude of the frequency itself. Further experiments could be performed to input the up and down spikes of the sigma-delta modulator in different forms to the neural populations, such as sending them to different neurons, and assess how this affects the spike-trains of irregular and regular neurons.

5 Conclusion

Our modeling approach demonstrated that by introducing uncorrelated noise into a neural population of inhibitory and excitatory neurons, the irregular neuron firing patterns of the vestibular system can be mimicked. Regular neuron populations can be generated as well on the Dynap-se chip without introducing uncorrelated noise and by tuning synaptic parameters. Adding stochastic connections in regular neuron populations could lead to more biologically-plausible behaviours in future experiments. In stimulus-free conditions, irregular and regular neuron populations of the vestibular system can be modeled on the Dynap-se chip. When imputing stimuli into the neuron populations, the methodology of the stimulus encoding, whether it follows an amplitude or rate encoding mechanism, alters the spike-train output of the neuron populations. We demonstrated that it is possible to reconstruct the input stimulus from Dynap-se neurons, up to a certain accuracy. According to our results, we conclude that the irregular neurons encode large changes in head-direction velocity and high frequency stimuli, whereas artificial regular afferents more faithfully encode the amplitude of the stimulus.

References

[1] Chicca, E., Fusi, S. (2001). Stochastic synaptic plasticity in deterministic aVLSI networks of spiking neurons. In F. Rattay (Ed.), Proceedings of the World Congress on Neuroinformatics (pp. 468-477). Vienna: ARGESIM/ASIM Verlag.

[2] Corradi, F., Zambrano, D., Raglianti, M., Passetti, G., Laschi, C., Indiveri, G. (2014). Towards a neuromorphic vestibular system. IEEE transactions on biomedical circuits and systems, 8(5), 669–680. https://doi.org/10.1109/TBCAS.2014.2358493

[3] Sadeghi SG, Chacron MJ, Taylor MC, Cullen KE. Neural variability, detection thresholds, and information transmission in the vestibular system. J Neurosci. 2007 Jan 24;27(4):771-81. doi: 10.1523/JNEUROSCI.4690-06.2007. PMID: 17251416; PMCID: PMC5053814.

[4] Purves D, Augustine GJ, Fitzpatrick D, et al., editors. Neuroscience. 2nd edition. Sunderland (MA): Sinauer Associates; 2001. Available from: https://www.ncbi.nlm.nih.gov/books/NBK10799/

[5] https://gist.github.com/fedden/d06cd490fcceab83952619311556044a

[6] https://code.ini.uzh.ch/ncs/libs/sp-delta-encoding-theory